Cooperative Robustness to Static Disorder: Superradiance and localization in a nanoscale ring to model natural light-harvesting systems

G. Luca Celardo,[1,2] Giulio G. Giusteri,[1,3] and Fausto Borgonovi[1,2]

[1]*Dipartimento di Matematica e Fisica and Interdisciplinary Laboratories for Advanced Materials Physics,
Università Cattolica del Sacro Cuore, via Musei 41, I-25121 Brescia, Italy*
[2] *Istituto Nazionale di Fisica Nucleare, Sezione di Pavia, via Bassi 6, I-27100, Pavia, Italy*
[3]*International Research Center on Mathematics & Mechanics of Complex Systems,
via XIX marzo 1, I-04012 Cisterna di Latina, Italy*
(Dated: July 4, 2021)

We analyze a 1-d ring structure composed of many two-level systems, in the limit where only one excitation is present. The two-level systems are coupled to a common environment, where the excitation can be lost, which induces super and subradiant behavior, an example of cooperative quantum coherent effect. We consider time-independent random fluctuations of the excitation energies. This static disorder, also called inhomogeneous broadening in literature, induces Anderson localization and is able to quench Superradiance. We identify two different regimes: *i*) weak opening, in which Superradiance is quenched at the same critical disorder at which the states of the closed system localize; *ii*) strong opening, with a critical disorder strength proportional to both the system size and the degree of opening, displaying robustness of cooperativity to disorder. Relevance to photosynthetic complexes is discussed.

PACS numbers: 71.35.-y, 72.15.Rn, 05.60.Gg

I. INTRODUCTION

Since the discovery that quantum coherences might have a functional role in biological systems even at room temperature [1–5], there has been great interest in understanding how coherences can be maintained and used under the influence of different environments with competing effects. In particular, much of recent research focused on one-dimensional nanostructures, due to their relevance to molecular aggregates, such as the J-aggregates [6], natural photosynthetic systems [7], bio-engineered devices for photon sensing [8] and light-harvesting systems [9].

Here we focus on a ring-like structure of two-level systems coupled with nearest neighbor tunneling amplitudes which has been recently considered in literature [7–12]. Usually, under low light intensity, in many natural photosynthetic systems or in ultra-precise photon sensors the single-excitation approximation can be used. In this case the system is equivalent to a tight binding model where one excitation can hop from site to site, see Fig. 1.

Many photosynthetic organisms contain ring-like chlorophyll molecular aggregates in their light-harvesting complexes, which are called LHI and LHII [13]. These complexes have the purpose to absorb light and to transfer the excitations to other structures or to a central core absorber, the reaction center, where charge separation, necessary in the next steps of photosynthesis, occurs. These complexes are subject to the effects of different environments: *i*) dissipative, where the excitation can be lost; *ii*) proteic, which induces static or dynamical disorder. The efficiency of excitation transfer can be determined only through a comprehensive analysis of the effects due to the interplay of all those environments.

Here, in particular, we consider a system subject to the influence of both a common decay channel where the excitation can be lost, and a static disorder. The first environment can be thought of as a model for the coupling of a molecular aggregate to the electromagnetic field [11] (loss of excitation by recombination) or for the coupling of the molecular aggregate to a central core absorber (loss of excitation by trapping). For many molecular aggregates, the single channel approximation is appropriate to describe the coupling with the electromagnetic field, since the wavelength of the absorbed light is much larger than the system size (natural complexes such as LHI, LHII typically span few tens of nanometers, while the wavelength of the involved photon is hundreds of nanometers). Moreover, it can also be considered as a good approximation for the coupling to a central core absorber, modeled for instance by a semi-infinite one-dimensional lead [14, 15].

The second environment consists of a protein scaffold, in which photosynthetic complexes are embedded, that induces fluctuations in the sites energies. The fluctuations which occur on a time scale much larger than the time scale of the dynamics are usually described as static disorder. By static disorder we mean position dependent, but time-independent, fluctuations of the site energies. The case of time-dependent fluctuations of site energies has been considered in a separate paper [16].

It is well known that, when many sites are all coupled to the same channel, we can have a superradiant behavior [17]. Superradiance implies the existence of some states with a cooperatively enhanced decay rate (i.e. proportional to the number of sites). Superradiance comes always together with Subradiance, that is the existence of states with a cooperatively suppressed decay rate (i.e. smaller than the single-site decay rate).

Though originally discovered in the context of atomic

clouds interacting with the electromagnetic field [18], in presence of many excitations, Superradiance was soon recognized to be a general phenomenon in open quantum systems [17] under the conditions of coherent coupling with a common decay channel. Most importantly, it can also occur in presence of a single excitation (the super of Superradiance [19]), entailing a purely quantum effect.

The functional role that Superradiance might have in natural photosynthetic systems has been discussed in many publications [5, 8, 20, 21], and experimentally observed in molecular aggregates [6, 22]. Superradiance (or Supertransfer) is also thought to play an important role w.r.t. the transfer of excitation to the central core absorber [5], and its effects on the efficiency of energy transport in photosynthetic molecular aggregates have been recently analyzed [23, 24].

The origin of Superradiance lies in the fact that the excitation can be coherently spread over several sites, thus inducing a cooperative effect. On the other hand, static disorder is expected to destroy Superradiance, since it induces Localization [25], which implies that excitons are localized on one site only, thus hindering cooperativity. The main question we want to address here is whether a critical disorder exists at which Superradiance and, thus, cooperativity are destroyed. The relation between Superradiance and Localization have been already analyzed in literature in different contexts [12, 26–28]. In particular, in [12] the case of weak coupling to the continuum (weak opening) has been analyzed for one-dimensional systems. It has been already analyzed also by some of the Authors of the present paper: in [27] the case of open 1-d and 3-d Anderson models in the strong opening regime was considered. It was pointed out there that the sensitivity to disorder can be very different for superradiant and subradiant states: while the latter localize at the same critical disorder of the closed system (i.e. a system with no coupling to the continuum of states), the former localize at the critical disorder for which Superradiance is quenched. Interestingly, though subradiant states essentially localize at the localization threshold associated with the closed system, they display some peculiar features due to opening, being neither fully localized nor extended (hybrid states) [27]. In this paper we aim to study both the regimes of weak and strong opening and their effects on Localization in one-dimensional nanostructures.

Even if it is easy to imagine that opening and disorder have competing effects on the efficiency of energy absorption and transfer, a deeper analysis is necessary to fully understand their action. For instance, disorder decreases the efficiency of the superradiant states in absorbing light or in transferring excitations, but, at the same time, it can allow for energy absorption and transfer from the subradiant states. Thus, for these states, disorder is useful to enhance efficiency. The latter effect is strongly related to the enhancement of efficiency due to noise: the so called noise-assisted transport, discussed in [29, 30]. Noise-assisted transport constitutes
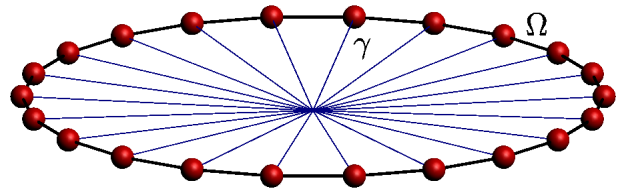

FIG. 1: (Color online) The ring model. One excitation can hop between N sites coupled with nearest-neighbors tunneling transition amplitude Ω. All sites are connected to a common decay channel, where the excitation can escape, with an equal coupling strength γ.

a general phenomenon in quantum networks, even if its relation with Subradiance has never been stressed up to now, to the best of our knowledge. The plan of the paper is the following: in Sec. II we introduce the model, in Sec. III we derive analytically the critical disorder strength needed to quench Superradiance, identifying the different regimes of weak and strong opening. In Sec. IV we analyze in detail the relation with Localization, while Sec. V is devoted to study the consequences of the previous findings on the system dynamics. A brief discussion about the relevance to photosynthetic complexes is given at the end of each Section.

II.   THE MODEL WITHOUT DISORDER

We considered a 1-d chain of sites with periodic boundary conditions, arranged to form a ring-like structure, as shown in Fig. 1, where the excitation can hop from site to site. The model is characterized by the following tight binding Hamiltonian:

$$H^{tb} = -\Omega \sum_{\langle i,j \rangle} \left(|j\rangle\langle i| + |i\rangle\langle j| \right) , \qquad (1)$$

where the summation index $\langle i,j \rangle$ runs over the pairs of nearest-neighbor sites and $\Omega > 0$ is the tunneling transition amplitude. Here $|j\rangle$ represents a state in which the excitation is at the site j, while all the other sites are unoccupied. In terms of two-level system states $(|0\rangle, |1\rangle)$ it can be written as

$$|j\rangle = |0\rangle_1 |0\rangle_2 \ldots |1\rangle_j \ldots |0\rangle_N .$$

The eigenvalues

$$E_q = -2\Omega \cos \frac{2\pi q}{N} \text{ with } q = 1, \ldots, N \qquad (2)$$

and the eigenstates $|\psi_q\rangle$ of the system can be computed exactly. Concerning the components of the eigenstate $|\psi_q\rangle$ on the site basis $|s\rangle$, one has

$$\langle s | \psi_q \rangle = \frac{1}{\sqrt{N}} \cos \frac{2\pi sq}{N}$$

for $q = 1, \ldots, N/2, N$, and

$$\langle s | \psi_q \rangle = \frac{1}{\sqrt{N}} \sin \frac{2\pi s(N-q)}{N}$$

for $q = N/2+1, \ldots, N-1$. The ground state, corresponding to $q = N$ and energy $E_N = -2\Omega$, is fully symmetric and extended in the site basis:

$$|\psi_N\rangle = \frac{1}{\sqrt{N}} \sum_{k=1}^{N} |k\rangle. \qquad (3)$$

The 1-d Anderson model can be "opened" by allowing the excitation to escape the system from any site into the same continuum channel. This situation of "coherent dissipation" can be met in many systems and it has been recently considered in [27], where it has been shown to give rise to the following effective non-Hermitian Hamiltonian (see also [15]):

$$(H_{\text{eff}})_{ij} = (H^{tb})_{ij} - \frac{i}{2} \sum_c A_i^c (A_j^c)^* \equiv (H^{tb})_{ij} - i\frac{\gamma}{2} Q_{ij}, \qquad (4)$$

where A_i^c are the transition amplitudes from the discrete state i to the continuum channel c. In our case, we have a single decay channel, $c = 1$, and equal couplings, $A_i^1 = \sqrt{\gamma}$, so that $Q_{ij} = 1 \ \forall i, j$.

The quantum evolution is given by the operator

$$\mathcal{U} = e^{-iH_{\text{eff}}t/\hbar},$$

which is non-unitary, and gives rise to a loss of probability in the decay channel. The complex eigenvalues of H_{eff} can be written as $E_r - i\Gamma_r/2$, where Γ_r represent the decay widths of the eigenstates. Usually, in molecular aggregates, energy is measured in units of cm^{-1}, corresponding to energy divided by hc. In these units, time is measured in cm which corresponds to the mapping $t \to 2\pi ct$ ($c \simeq 0.03$ cm/ps is the speed of light). In the following all units of energy will be given in cm^{-1} and in order to have time in ps we need to divide it by $2\pi c$.

Due to its specific structure, the operator Q has only one eigenstate with a non-zero eigenvalue: this is the fully extended state with eigenvalue equal to N. This eigenstate also corresponds to the ground state of H^{tb}, given in Eq. (3). All the other eigenstates of Q are degenerate with null eigenvalue and, since $[Q, H^{tb}] = 0$, they can be chosen to match the eigenstates $|\psi_q\rangle$, $q < N$, of H^{tb}. This implies that only the state $|\psi_N\rangle$, Eq. (3), has a non-vanishing decay width equal to the total decay width of the system: $\Gamma_N = N\gamma$. This is the superradiant state. Note that the dependence on N of that decay width is the hallmark of the cooperative nature of Superradiance. All the other states with zero decay width are called subradiant. The full expression for the complex eigenstates of the non-Hermitian Hamiltonian, Eq.(4), is given in Appendix A, see Eq.(A2). Importantly, the superradiant effect might explain the strong dependence on the initial state of the efficiency of energy transfer to a central core absorber discussed in Ref. [10].

Several features of the model above in absence of disorder are quite atypical. Indeed, Superradiance, as discussed in many papers [17, 31], is usually reached only above a critical coupling strength with the continuum (in the overlapping resonance regime) when

$$\langle\Gamma\rangle/\Delta \geq 1, \qquad (5)$$

where $\langle\Gamma\rangle$ is the average decay width and Δ is the mean level spacing of the closed system. On the other hand, *we are in a superradiant regime for any $\gamma > 0$*, even if the overlapping resonance condition is not satisfied. Moreover, the widths of the subradiant states are usually small, but not zero as in this case. This is also due to the particular symmetric configuration chosen, from which it follows that H^{tb} and Q commute. Note that such geometrically-induced subradiant subspaces with zero decay width are equivalent to the trapping-free subspaces discussed in literature [30].

Finally, let us notice that the presence of a superradiant regime for any coupling strength to the continuum might indicate a relation between structure and function in natural complexes, and it might also suggest the use of ring-like structures to exploit the superradiant behavior.

III. SUPERRADIANCE AND ANALYSIS OF DECAY WIDTHS IN PRESENCE OF DIAGONAL DISORDER

The peculiar features discussed above disappear when we introduce the diagonal disorder, described by adding to the Hamiltonian, Eq. (4), the term

$$D = \sum_{j=1}^{N} \epsilon_j |j\rangle\langle j|, \qquad (6)$$

where the random diagonal energies ϵ_j are taken uniformly distributed in $[-W/2, +W/2]$, W being the disorder strength. With the addition of this term our model becomes equivalent to a 1-d open Anderson model as considered in Ref. [27].

The presence of static disorder on the site energies breaks the symmetry of the system under rotations, inducing the width of the superradiant state to decrease and the widths of the subradiant states to increase (the total decay width $N\gamma$ is a constant that does not depend on the degree of disorder W), so that all of the eigenstates can decay into the continuum channel.

The effect of static disorder on the decay widths has been analyzed in Fig. 2, where the width of the superradiant state and the average width of all subradiant states are shown as a function of the disorder strength W, for different parameters value. As one can see, for small disorder, the effect on subradiant states is much more evident than that on the superradiant state. For large disorder, all widths approach the value γ, corresponding to the decay width of an isolated site. In this regime there is no collective behavior anymore and Superradiance is completely quenched.

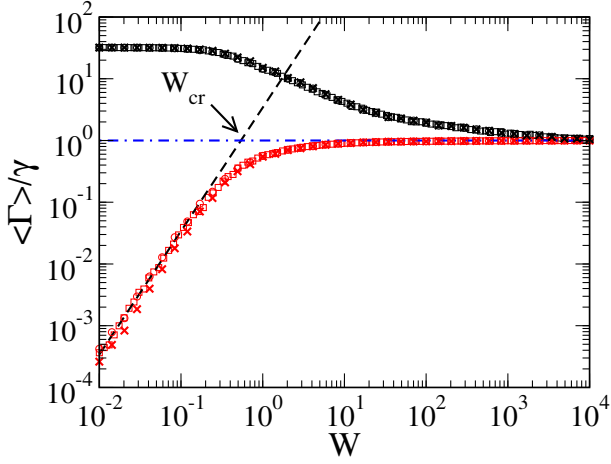For small disorder, it is possible to use perturbation theory (see Appendix A) to obtain the mean decay width

FIG. 2: (Color online) Average decay widths for a ring with $N = 32, \Omega = 1$ vs the disorder strength, W, for $\gamma = 10^{-4}$ (circles), $\gamma = 10^{-3}$ (squares), and $\gamma = 2 \times 10^{-3}$ (crosses). Black symbols (upper curve) refer to the average over disorder of the largest width (the superradiant state). Red symbols (lower curve) refer to the average over disorder of the mean subradiant width (mean taken over the $N-1$ smallest widths) $\langle\Gamma_{sub}\rangle$. As a dashed line we plot the perturbative result, Eq. (7), for $\langle\Gamma_{sub}\rangle$. The horizontal dot-dashed line indicates the value $\langle\Gamma\rangle = \gamma$. The critical disorder strength, Eq. (11), is indicated as the intersection between the line given by perturbation theory and the horizontal line, see text for details.

of the $N-1$ smallest widths:

$$\langle\Gamma_{sub}\rangle = \frac{\gamma W^2}{48\Omega^2(N-1)}$$
$$\times \sum_{q=1}^{N-1} \left[\left(\cos\frac{2\pi q}{N} - 1\right)^2 + \frac{N^2\gamma^2}{16\Omega^2}\right]^{-1}. \quad (7)$$

The sum in Eq. (7) can be well approximated in different parameter regimes to give (see Appendix B)

$$\langle\Gamma_{sub}\rangle = \begin{cases} \dfrac{\gamma W^2 N^3}{96\pi^4\Omega^2} & \text{for} \quad \dfrac{N\gamma}{2} \ll \delta E_{min}, \\[12pt] \dfrac{\gamma^{1/2}W^2}{12\Omega^{1/2}N^{3/2}} & \text{for} \quad \delta E_{min} \ll \dfrac{N\gamma}{2} \ll 2\Omega, \\[12pt] \dfrac{W^2}{3N^2\gamma} & \text{for} \quad \dfrac{N\gamma}{2} \gg 2\Omega. \end{cases} \quad (8)$$

Let us name *weak opening* the regime characterized by $N\gamma/2 \ll \delta E_{min}$ and *strong opening* the one in which $N\gamma/2 \gg 2\Omega$. The different regimes shown above can be understood if we consider that

$$\delta E_{min} = E_{N-1} - E_N \simeq 4\Omega\pi^2/N^2$$

is the minimal nearest neighbor energy distance, see Eq. (2). In Ref. [12] a perturbative result was obtained in the regime of weak opening, $N\gamma/2 \ll \delta E_{min}$, which agrees with our findings. As one can see from Eq. (8), the average subradiant width in any regime increases as

W^2, but the dependence on the system size, N, and on the degree of opening, γ, changes: in the weak opening regime, the widths increase with N and γ, whereas, for very strong opening, they decrease with N and γ.

In Fig. 2 the perturbative expression is shown as a dashed line and agrees very well with numerical data. From Eq. (7) one can define a critical disorder strength, W_{cr}, at which Superradiance is quenched, given by the condition

$$\langle\Gamma_{sub}(W_{cr})\rangle = \gamma, \quad (9)$$

from which one gets

$$W_{cr} = \sqrt{\frac{48\Omega^2(N-1)}{\sum_{q=1}^{N-1}\left[\left(\cos\frac{2\pi q}{N} - 1\right)^2 + \frac{N^2\gamma^2}{16\Omega^2}\right]^{-1}}}. \quad (10)$$

For $W \gg W_{cr}$, all of the widths become essentially the same and equal to γ, while below W_{cr} they strongly depend on the chosen state. Usually, the transition between these two regimes, which corresponds also to a transition from a non-cooperative to a cooperative regime, is referred to as Superradiance Transition (ST) in literature [17, 31].

Even if the validity of Eq. (10) has been shown in Fig. 2 only in the weak opening regime, we checked that it gives an excellent estimate of the disorder at which Superradiance is quenched also for strong opening.

From Eq. (10) it is possible to get an approximate expression (see Appendix B) for the critical disorder strength, W_{cr}, in the different regimes:

$$W_{cr} = \begin{cases} \sqrt{96}\pi^2\Omega N^{-3/2} & \text{for} \quad \dfrac{N\gamma}{2} \ll \delta E_{min}, \\[12pt] \sqrt{12}(\gamma\Omega N^3)^{1/4} & \text{for} \quad \delta E_{min} \ll \dfrac{N\gamma}{2} \ll 2\Omega, \\[12pt] \sqrt{3}N\gamma & \text{for} \quad \dfrac{N\gamma}{2} \gg 2\Omega. \end{cases} \quad (11)$$

The results contained in Eq. (11) are very interesting, since they show that in some region of parameters (typically small system size and weak opening) the critical disorder at which Superradiance is quenched is independent of γ (a quantity often difficult to be experimentally determined), while it decreases with the system size as $N^{-3/2}$. This independence from γ is also shown in Fig. 2 where we plotted data obtained with different values of γ, for which $N\gamma/2 \leq \delta E_{min}$. In particular, for the largest value of γ considered in Fig. 2, $\gamma = 2 \times 10^{-3}$, we have $N\gamma/2 \simeq \delta E_{min}$. The existence of a regime (weak opening) in which the critical disorder strength is independent of γ could be surprising. Indeed, applying the overlapping resonance criterion, Eq. (5), one would obtain $W_{cr} \propto \gamma$, since $\langle\Gamma\rangle \propto \gamma$ and $\Delta \propto W$. An explanation of this effect, due to Localization, will be given in the next Section.

A second remarkable result is the linear dependence of W_{cr} on N and γ in the strong opening regime. Since,
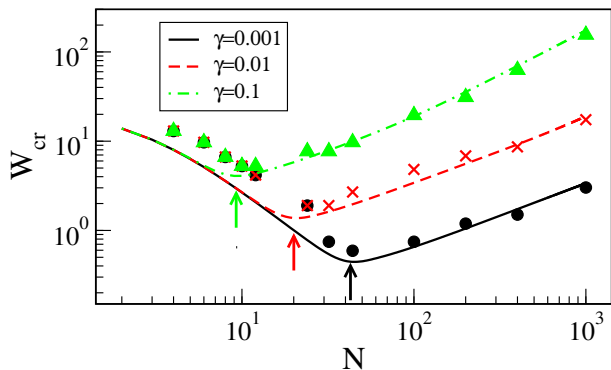
FIG. 3: (Color online) Disorder strength at which the variance of the decay widths have a maximum *vs* the number N of sites in the ring for different values of the coupling strength γ, as indicated in the legend. The numerical data (symbols) are compared with the analytical expression (curves) for the critical disorder strength, Eq. (10). Arrows indicate the size N_{cr} at which critical disorder is minimal, see Eq. (12).

on increasing N, one always enters the strong opening regime, it is possible to preserve the cooperative nature of superradiant states up to arbitrarily large disorder. We may thus say that the opening induces a cooperative robustness to disorder, as was also recently found by some of the Authors of this paper [27].

It is interesting to observe that also in the case of dynamical disorder it was found [16] that the critical dephasing necessary to destroy the cooperative superradiant effects is proportional to both N and γ. Note that this regime was not analyzed in Ref. [12], where it was stated that the critical disorder needed to quench Superradiance does not depend on the superradiant decay rate.

From Eq. (11) we can infer that the dependence of W_{cr} on the system size N is non-monotone. Setting $N\gamma/2 = \delta E_{min}$, we can roughly estimate the N value at which W_{cr} has a minimum:

$$N_{cr} \simeq \left(\frac{8\pi^2\Omega}{\gamma}\right)^{1/3}. \qquad (12)$$

To confirm the validity of the critical disorder strength, W_{cr}, computed above, as the value at which the ST occurs, we computed the variance of the decay widths. Indeed, it is well known [31] that, at the ST, the variance of the widths has a maximum. The results of such a comparison are presented in Fig. 3, showing a good agreement between the two estimates of the ST.

Finally, it is interesting to estimate the value of W_{cr} for the photosynthetic complexes LHI and LHII. In this case $\Omega \approx 600\,\text{cm}^{-1}$ and $N = 32$, 16, respectively [5, 13]. The coupling with the electromagnetic field can be estimated from the radiative decay time τ of a single molecule, which is of the order of few nanoseconds [13]. Hence we get $\gamma = 1/(2\pi c\tau) \approx 10^{-3}\,\text{cm}^{-1}$. On the other side, for the LHI complex, the common decay channel can also represent the reaction center. This coupling can be es-

timated to be $\gamma \approx 10^{-2}\,\text{cm}^{-1}$ from the mean transfer time to the reaction center of the LHI complex [13], as discussed at the end of Sec. V. Both these couplings are very weak if compared to the energy scale of Ω, so that we can assume that we are in a weak opening regime, $N\gamma/2 \ll \delta E_{min}$, where W_{cr} does not depend on γ and it will then be the same for both environments. We can thus use $W_{cr} = \sqrt{96}\pi^2\Omega N^{-3/2}$, see Eq. (11), getting $W_{cr} \approx 320\,\text{cm}^{-1}$ for LHI and $W_{cr} \approx 900\,\text{cm}^{-1}$ for LHII. These values of disorder are in agreement with the experimental observation that static disorder in LHII complexes is 2–3 times larger than the value of disorder in LHI complexes [22]. Those values are also quantitatively compatible with the estimated ranges of static disorder strength in natural photosynthetic complexes (100–600 cm^{-1} for LHI complexes [10, 22], 600–1400 cm^{-1} for LHII complexes [5, 13, 22]. To make a comparison with the data contained in these references, one should take into account that they considered Gaussian static disorder with a standard deviation σ, so that $W = \sqrt{12}\sigma$). These estimates might suggest that natural photosynthetic complexes operate close to the ST.

IV. SUPERRADIANCE AND LOCALIZATION

In the previous Section we analyzed how diagonal disorder modifies the decay widths of the states. On the other hand, it is well known that disorder in isolated tight binding models induces Anderson Localization [25]. In 1-d systems any disorder strength induces localized eigenstates, $|\langle j|\psi\rangle| \simeq \exp(-|j-j_0|/\xi)$, where j labels the position of the sites on the lattice and ξ is the localization length, measured in units of intersite distance. The localization length is, in general, a function of the disorder strength W and of the energy E. In particular, it is well known that, for weak disorder and away from the edges of the energy band, $\xi \propto W^{-2}$.

Therefore, it is possible to define a critical disorder W_d for the localization effect to be important by the simple equation

$$\xi(W_d) = N. \qquad (13)$$

Indeed, while any increase of the disorder strength will produce eigenstates with a localization length smaller than the sample size, decreasing W gives rise to eigenstates with a localization length larger than the system size, i.e. effectively delocalized.

The interplay of disorder and opening can be studied by means of the participation ratio

$$PR = \left\langle \frac{\sum_i |\langle i|\psi\rangle|^2}{\sum_i |\langle i|\psi\rangle|^4} \right\rangle \qquad (14)$$

of the eigenstates $|\psi\rangle$ of H_{eff}, given in Eq. (4), where $\langle\ldots\rangle$ stands for the ensemble average over different realizations of the static disorder. The PR is widely used to characterize localization properties [32] and it clearly satisfies the bounds $1 \leq PR \leq N$. For extended states,
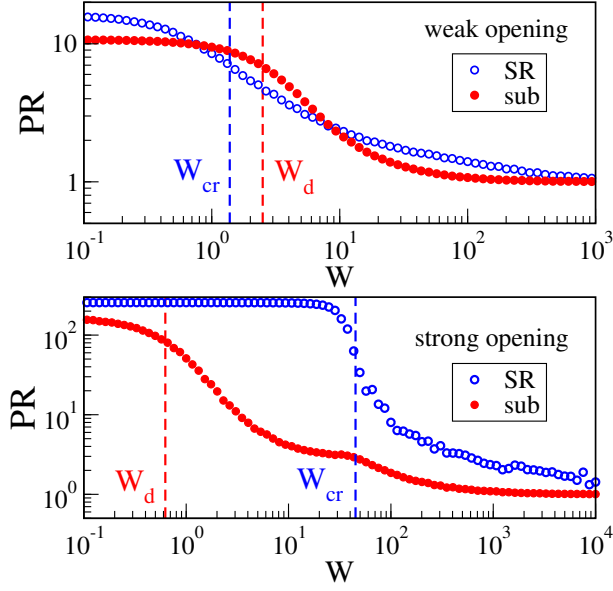
FIG. 4: (Color online) Average participation ratio PR vs the disorder strength W. Upper panel represents the weak opening regime, namely $N = 16, \gamma = 10^{-3}, \Omega = 1$, while the lower panel depicts the strong opening regime, $N = 256, \gamma = 10^{-1}, \Omega = 1$. In both panels the blue open circles represent the behavior of the superradiant state as a function of the disorder strength, while the red full circles stand for the average PR of the subradiant states. Vertical dashed lines represent in both panels the localization condition given by Eq. (13) (red), and W_{cr} (blue, Eq. (11)).

FIG. 5: (Color online) Disorder strength at which the PR decreases its value by 3% with respect to the value at $W = 0$, as a function of the system size, N, for the superradiant state (upper panel) and for the average PR over all the other states (lower panel). Circles stand for the open system ($\gamma = 0.001$), crosses for the closed system ($\gamma = 0$). Here is $\Omega = 1$. In the upper panel the full curve stands for the analytical W_{cr}, given by Eq. (11), rescaled by a factor 8 to fit numerical data. In the lower panel a curve proportional to $N^{-1/2}$ has been drawn to guide the eye (for the explanation see text). Vertical dashed lines mark N_{cr}, see Eq. (12), and separate the weak opening regime (left) from the strong opening regime (right).

it increases proportionally to the system size N, while, for localized states, it is independent of N.

Our aim is to compare the disorder strength at which Superradiance is quenched, W_{cr}, see Eq. (10), with the disorder strength at which the states localize, W_d, see Eq. (13). To do that, we analyze separately the PR of the superradiant state (the state with the maximum decay width) and the average PR of the other $N - 1$ states as a function of W.

The typical behavior of the PR as a function of the disorder strength W has been analyzed in Fig. 4 in two different situations: for weak opening ($N\gamma/2 \ll \delta E_{min}$, upper panel), and for strong opening ($N\gamma/2 \gg 2\Omega$, lower panel). In both cases, the PR of the superradiant state decreases roughly at the ST, as given by W_{cr}, while the PR of subradiant states decreases roughly at W_d.

To be more quantitative, we numerically computed, for the superradiant state and for the subradiant states, the disorder strength W_{PR} at which their PR decreases by 3% w.r.t. the value at zero disorder. To highlight the peculiar effects due to opening, these results should be compared with those for the closed system ($\gamma = 0$). For the closed system we cannot define superradiant and subradiant states, but, since the localization length depends on the energy level, we can compare states of the open system with states of the closed system having the same real energy. In particular, the superradiant state is
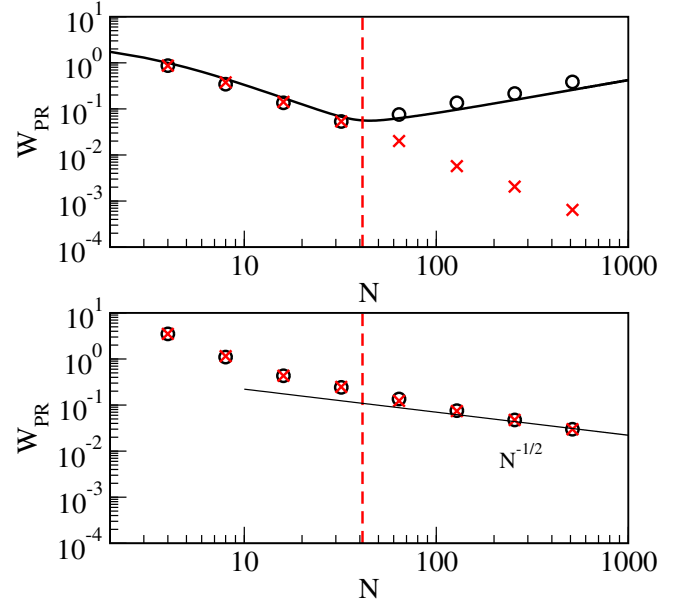
compared with the ground state of the closed system.

Results are shown in Fig. 5 for the superradiant state (upper panel) and for the subradiant ones (lower panel) as a function of the system size N. In this Figure we fix γ and, by varying N, we switch from the weak opening regime (for small N values) to the strong opening regime (for large N). The N_{cr} value which separates the two different regimes can be estimated from Eq. (12), and has been indicated as a dashed vertical line in both panels.

The opening does not modify the behavior of the subradiant states if compared with the behavior of the closed system, compare circles with crosses in the lower panel of Fig. 5. In particular, for non-edge states of the closed system [33] $\xi \simeq 100/W^2$, and, from Eq. (13), one gets that the disorder strength at which states localize scales as $N^{-1/2}$. The same dependence on N is found in presence of opening and it has been indicated for the sake of comparison in Fig. 5, lower panel.

Let us now analyze the behavior of superradiant states, Fig. 5 upper panel. In the weak opening regime, $N < N_{cr}$, the open and the closed model display the same behavior, while in the strong opening regime, $N > N_{cr}$, the behavior is very different: in this regime W_{PR} decreases with N for the closed model, while it increases with N

for the open one.

Even if the behavior of the superradiant state of the open system in the weak and strong opening regimes is very different, it is always captured by the disorder strength at which Superradiance is quenched, W_{cr}, see Eq. (11). Indeed, the disorder strength at which the superradiant state starts lo localize (phenomenologically described by W_{PR}) scales with the parameters as W_{cr} (compare full line with symbols in upper panel of Fig. 5). This fact allows us to understand the scaling of W_{PR} with N in both regimes: $W_{PR} \propto N^{-3/2}$ in the weak opening regime, while $W_{PR} \propto N$ in the strong opening regime.

Note that the dependence $W_{PR} \propto N^{-3/2}$ is the same as that of the disorder strength necessary to localize the edge states of the closed system [34], for which we have $\xi(W) \propto W^{-2/3}$ and, from Eq. (13), we obtain a disorder strength scaling as $N^{-3/2}$.

The different sensitivity of super and subradiant states to disorder is far from being trivial. Due to the fact that the Q matrix in Eq.(4) is a full matrix, the opening induces a long-range hopping which contrasts localization, and one might expect such long range to affect all states equally. On the other hand, the correlated nature of the long range hopping implies that only superradiant states are affected, leaving the subradiant states effectively decoupled from the environment and thus behaving more similarly to the states of the closed system. For more details see Ref. [27].

Summarizing we can conclude that:

- the disorder strength necessary to localize the subradiant states is the same of the corresponding value for the closed system;

- the disorder strength necessary to localize the superradiant states is proportional to the disorder strength necessary to quench Superradiance, W_{cr};

- in the weak opening regime, the quenching of Superradiance is determined only by the Localization properties of the closed model, resulting in a W_{cr} independent of γ;

- in the strong opening regime, Superradiance is quenched at a critical disorder proportional to $N\gamma$, as in the case of time-dependent disorder [16], thus showing its cooperative robusteness to disorder;

- for the realistic parameters of natural photosynthetic complexes, such as LHI and LHII (see end of Sec. III), we are in the weak opening regime, so that it is possible to determine W_{cr} only by analyzing the localization properties of the closed system. This fact can be very useful since the exact value of γ is not easy to be determined experimentally.
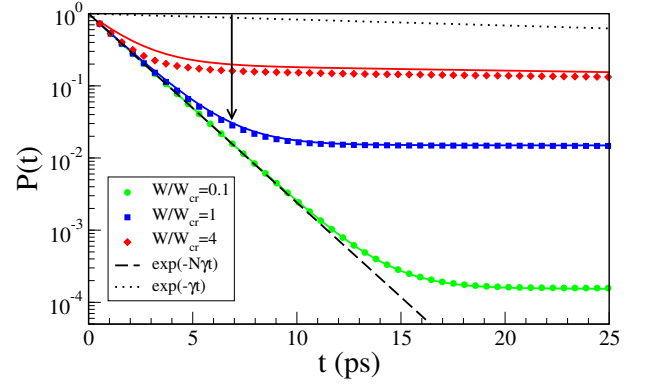

FIG. 6: (Color online) Time evolution of the survival probability starting from the fully extended state. We set $N = 32$, $\gamma = 0.1$, $\Omega = 1$, for different disorder strengths as indicated in the legend. Numerical results are shown with symbols, while full curves show the analytical expression, Eq. (16). The arrow shows the value of $t^\star$ obtained analytically by Eq. (17) for $W = W_{cr}$. For comparison, both the exponential decay of the superradiant state for zero disorder (dashed) and the decay at large disorder (dotted) are shown.

V. DYNAMICS OF THE SURVIVAL PROBABILITY

In this Section we aim at studying how the time evolution of the survival probability $P(t)$ (that is the probability of finding the excitation in the system, initially prepared in some state $|\psi_0\rangle$) is modified by the presence of static disorder. That quantity is given by

$$P(t) = \sum_{k=1}^{N} |\langle k|e^{-iH_{\text{eff}}t/\hbar}|\psi_0\rangle|^2. \tag{15}$$

Let us choose $|\psi_0\rangle = |\psi_N\rangle$, the fully extended state of Eq. (3), for our first analysis. For $W = 0$ we clearly have $P(t) = e^{-N\gamma t}$, since the fully extended state is the only one with a decay width, see Eq.(A2). For $W \neq 0$ the fully extended state does not coincide with the superradiant state anymore, and it should be written as a superposition of superradiant and subradiant states. Using first order perturbation theory (in the disorder strength W) we can derive an approximate expression for $P(t)$ valid for small time, see Appendix A, Eq. (A8):

$$P(t) \approx c_1 e^{-N\gamma t} + (1 - c_1)e^{-\Gamma_{sub}^{max}t}. \tag{16}$$

Eq. (16) takes into account only the superradiant decay and the fastest subradiant decay, Γ_{sub}^{max}, which can be computed from Eq. (A6) given in Appendix A, setting $q = N - 1$.

In Fig. 6 we compared numerical data for $P(t)$ with the analytical expression given in Eq. (16): the agreement is excellent for disorder strength $W < W_{cr}$, where the decay is well approximated by a bi-exponential function. From Eq. (16) it is also possible to compute the time at which a change in the decay occurs, t^*, by equating the two terms on the r.h.s. of Eq. (16). Dividing by $2\pi c$ in order
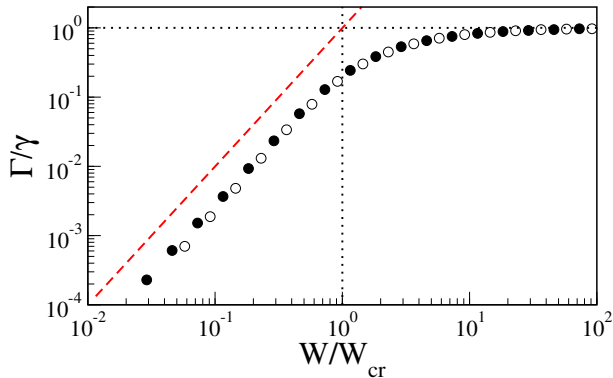
FIG. 7: (Color online) Inverse Decay time of the average probability $\langle P(t) \rangle$, rescaled to the individual decay width γ, as a function of the rescaled disorder strength W/W_{cr}. Different sets of values have been considered: full circles are for $N = 20$, $\gamma = 2.5$, $\Omega = 0.5$, $W_{cr} = 86.6$; open circles are for $N = 100$, $\gamma = 0.1$, $\Omega = 0.1$, $W_{cr} = 17.32$. The dashed red line represents $\langle \Gamma_{sub} \rangle = \gamma$.

to have t^* in picoseconds, we obtain

$$t^* = \frac{1}{2\pi c(N\gamma - \Gamma_{sub}^{max})} \log\left(\frac{c_1}{1 - c_1}\right). \qquad (17)$$

Such a time, for one value of the disorder strength, is shown with an arrow in Fig. 6. Note that t^* can be considered as the time up to which the decay is superradiant. As the disorder increases, t^* goes to zero and the decay of the extended state becomes similar to the decay of independent sites, i.e. $P(t) = e^{-\gamma t}$.

The generality of our results can be assessed by observing that the critical disorder at which Superradiance is quenched is an important threshold for the whole system dynamics and not only for the superradiant state. To this end, let us consider as initial state a random superposition of site states

$$|\psi_0\rangle = \sum_{k=1}^{N} c_k |k\rangle,$$

c_k being random complex coefficients such that $\sum_{k=1}^{N} |c_k|^2 = 1$. For such initial state, we compute the survival probability $P(t)$, for one realization of disorder. By changing the random initial state and the random diagonal disorder, we can consider the average survival probability $\langle P(t) \rangle$ and define the decay time $\tau \equiv 1/\Gamma$ as

$$\langle P(\tau) \rangle = 1/e.$$

These Γ values are reported in Fig. 7 as a function of W/W_{cr} for different parameter values. For the sake of comparison we show, in the same figure, the analytical expression for the average decay width of the subradiant states, see Eq. (10). As one can see, up to a numerical constant, the agreement is very good. In other words, the disorder strength necessary to quench Superradiance (obtained analytically imposing the average decay width

of the subradiant states, $\langle \Gamma_{sub} \rangle$, to be equal to the single site decay γ) is also a valid tool in estimating the decay time of the survival probability associated with generic random initial conditions.

The problem of computing the survival probability of the superradiant state in presence of inhomogeneous broadening was also considered in [35] for N two-level systems. A bi-exponential behavior was numerically found for any excitation number. For the case where only one excitation is present, our results are compatible with the bi-exponential behaviour of the survival probability found in [35], and we also give an approximate analytical expression for the survival probability $P(t)$.

Finally, in order to stress the relevance of superradiant energy transfer in natural photosynthetic complexes, let us consider the excitation transfer from the LHI complex to the reaction center [5, 13]. First of all, we point out that all models used to study the dynamics of this complex are characterized by a large inhomogeneity in the transfer time of different energy eigenstates [5, 10, 13], which is, for instance, typical of the superradiant regime. Thus, we reasonably assume Superradiance in transfer to be relevant in natural complexes. We can estimate γ, representing the coupling to the reaction center, from the following considerations. Using realistic parameters as was done at the end of Sec. III, $\Omega \approx 600 \, \text{cm}^{-1}$, $N = 32$, we computed $P(t)$ for the fully extended state of Eq. (3), in presence of a realistic value of the static disorder $W = 320 \, \text{cm}^{-1}$ (a large disorder corresponding to the critical disorder at which Superradiance starts to be quenched). We choose $\gamma = 0.01 \, \text{cm}^{-1}$, so that we have a transfer time (time at which $P(t) = 1/e$) starting from the fully extended state of $\approx 35 \, \text{ps}$, in agreement with experimental data [13]. Note that a single occupied site would give a transfer time of $500 \, \text{ps}$, showing that, even in presence of strong and realistic static disorder, Superradiance is able to strongly enhance energy transfer.

VI. CONCLUSIONS

We analyzed the interplay of Superradiance, induced by the coupling to a common decay channel, and Localization, induced by static disorder, in 1-d ring-like structures, usually used to model some natural light-harvesting complexes. The common decay channel can represent both the coupling to the electromagnetic field or to a central core absorber, such as the reaction center in natural photosynthetic complexes. We have shown that, for zero disorder, these structures are in a superradiant regime for any value of the coupling strength to a common decay channel. Above a critical disorder strength superradiant effects decrease until, for very large disorder, all of the states decay independently with the common width γ, and cooperativity is completely lost. Our main purpose was to determine the critical disorder at which Superradiance is hindered. Using a perturbative approach we determined analytically such critical disor-

der and we related it firstly with the localization properties of superradiant and subradiant states and then to the system dynamics. We found that Superradiance can be quenched by disorder in different ways, depending on the regime entailing either weak or strong coupling to the continuum. These regimes are triggered by the parameter $N\gamma/4\Omega$, which represents the ratio between the coupling strength to the continuum, γ, and the unperturbed mean level spacing in absence of disorder, $4\Omega/N$. When this ratio is small, i.e. $N\gamma/4\Omega \ll 2(\pi/N)^2$, the critical disorder is independent of the coupling strength with the external environment and it is determined only by the parameters of the molecular chain, since the opening is unable to affect the disorder-induced Localization. In this regime, the critical disorder decreases with the size of the system, but, for large system size $N \to \infty$, such a regime becomes less and less feasible (to be in the weak opening regime implies the condition $N^3 \ll 8\pi\Omega/\gamma$). On the other hand, for strong opening, $N\gamma/4\Omega \gg 1$, the critical disorder increases with both the size of the system and the coupling strength with the external environment. This is in agreement with the results recently found in Ref. [16], where the same ring structure has been analyzed in presence of dephasing (dynamical disorder) and the strength necessary to destroy Superradiance was found to be proportional to both γ and N.

We also demonstrated that the critical disorder at which Superradiance is suppressed is close to the disorder at which superradiant states localize [27]. Specifically, we found that, in the weak opening regime, $N\gamma/4\Omega \ll 2(\pi/N)^2$, Superradiance is quenched at the same disorder at which the edge state of the closed system, with real energy equal to that of the superradiant state, localizes.

We have also found that, in the strong opening regime, $N\gamma/4\Omega \gg 1$, Superradiance is a manifestation of cooperative robustness to disorder, in that the superradiant state localizes at a disorder strength (proportional to the system size) much larger than the one needed to localize the corresponding edge state of the closed system. As for subradiant states, in any regime, they begin their process of localization at the same disorder strength at which the states of the closed system do.

Finally, we have shown the relevance of our findings to natural photosynthetic complexes: *i)* for the realistic parameters of natural complexes, Superradiance is quenched at a disorder strength which is independent of the coupling to the external environment (electromagnetic field or reaction center), which is difficult to determine experimentally. Thus our findings allow to determine the critical disorder from the localization properties of the closed system alone; *ii)* the critical disorder thus obtained is compatible with experimental estimates, suggesting that natural systems operate close to the Superradiance Transition; *iii)* even in presence of large and realistic static disorder, Superradiance can strongly enhance energy transfer to the reaction center and light absorbtion.

Appendix A: Decay widths, a perturbative approach

Perturbation theory is applied to the *symmetric unperturbed Hamiltonian, $H^{tb} - i\gamma Q/2$*, in order to find the critical disorder strength, W_{cr}, at which Superradiance is destroyed. Let us rewrite the Hamiltonian given in Eq. (4) as

$$H_{\text{eff}} = H^{tb} - \frac{i\gamma}{2}Q + D,$$

where H^{tb} is the tight binding Hamiltonian, Eq. (1), in absence of disorder and $D = \sum_i \epsilon_i |i\rangle\langle i|$, see Eq. (6), is a diagonal matrix which contains the disordered site energies ϵ_i.

It is necessary to define the non-Hermitean "bra" as the transposed of a ket

$$\langle\langle\psi| := (|\psi\rangle)^t,$$

while the standard bra is the adjoint

$$\langle\psi| := (|\psi\rangle)^\dagger.$$

Indeed, given the right eigenvectors of a symmetric Hamiltonian $|\psi_i\rangle$, the left eigenvectors are $\langle\langle\psi_i|$, that is

$$H |\psi_i\rangle = \mathcal{E}_i |\psi_i\rangle, \qquad \text{and} \qquad \langle\langle\psi_i| H = \mathcal{E}_i \langle\langle\psi_i|,$$

and we have the *biorthogonality* condition

$$\langle\langle\psi_i|\psi_j\rangle = \delta_{ij}.$$

Clearly, for real eigenstates we have $\langle\langle\psi| = \langle\psi|$.

Matrix elements of the operators defined above, in the site basis $\{|s\rangle, s = 1, \ldots, N\}$, are given by,

$$D_{ss} = \epsilon_s, \quad H^{tb}_{1N} = H^{tb}_{ss+1} = -\Omega, \quad Q_{sr} = 1, \quad \text{(A1)}$$

with $r, s = 1, \ldots, N$. In Eq. (A1) $\Omega > 0$, and $-W < \epsilon_s < W$, are independent identically distributed random variables with mean 0 and variance $W^2/12$.

Since $[H^{tb}, Q] = 0$, it is convenient to study the whole system on the basis of eigenstates of H^{tb}, which are given by

$$\langle s|\psi_q\rangle = \frac{1}{\sqrt{N}} \cos\frac{2\pi sq}{N}$$

for $q = 1, \ldots, N/2, N$, and

$$\langle s|\psi_q\rangle = \frac{1}{\sqrt{N}} \sin\frac{2\pi s(N-q)}{N}$$

for $q = N/2 + 1, \ldots, N - 1$, with eigenvalues

$$e_q = -2\Omega \cos\frac{2\pi q}{N}.$$

The eigenvalues of the Hamiltonian, $H^{tb} - (i/2)\gamma Q$, are thus given by,

$$\varepsilon_q = -2\Omega \cos\frac{2\pi q}{N} - (iN\gamma/2)\delta_{qN}, \qquad \text{(A2)}$$

that is, only the ground state acquires a decay width $N\gamma$. Such a state is called *superradiant,* and the others are *subradiant.* Notice that $|\psi_N\rangle$ and $|\psi_{N/2}\rangle$ are non-degenerate, while, for any $q = 1, \ldots, N/2 - 1$, $|\psi_q\rangle$ and $|\psi_{N-q}\rangle$ span a two-dimensional degenerate eigenspace.

When the disorder strength is turned on every state will get an eigenenergy with a negative imaginary part (decay width). Perturbation theory up to second order can be applied, for sufficiently small disorder strength, to give

$$
\varepsilon'_q = \varepsilon_q + \langle\langle\psi_q \,|\, D \,|\psi_q\rangle\rangle + \sum_{q' \neq q} \frac{\langle\langle\psi_q \,|\, D \,|\psi_{q'}\rangle\rangle^2}{\varepsilon_q - \varepsilon_{q'}}
$$

$$
= \varepsilon_q + \sum_{s=1}^N \epsilon_s \langle s \,|\psi_q\rangle^2 \qquad (A3)
$$

$$
+ \sum_{s,s'=1}^N \sum_{q' \neq q} \frac{\epsilon_s \epsilon_{s'} \langle\langle\psi_q\,|s\rangle \langle s\,|\psi_{q'}\rangle \langle\langle\psi_{q'}\,|s'\rangle \langle s'\,|\psi_q\rangle}{\varepsilon_q - \varepsilon_{q'}} .
$$

For degenerate energy levels the first order correction is given by the eigenvalues of the 2 by 2 symmetric matrices

$$
\begin{pmatrix} \langle\langle\psi_q \,|\, D \,|\psi_q\rangle\rangle & \langle\langle\psi_q \,|\, D \,|\psi_{N-q}\rangle\rangle \\ \langle\langle\psi_{N-q} \,|\, D \,|\psi_q\rangle\rangle & \langle\langle\psi_{N-q} \,|\, D \,|\psi_{N-q}\rangle\rangle \end{pmatrix} =
$$

$$
= \begin{pmatrix} \sum_s \epsilon_s \langle s\,|\psi_q\rangle^2 & \sum_s \epsilon_s \langle s\,|\psi_{q'}\rangle \langle s\,|\psi_q\rangle \\ \sum_s \epsilon_s \langle s\,|\psi_{q'}\rangle \langle s\,|\psi_q\rangle & \sum_s \epsilon_s \langle s\,|\psi_{q'}\rangle^2 \end{pmatrix} \quad (A4)
$$

while the second order correction is

$$
\sum_{s,s'=1}^N \sum_{q' \neq q, N-q} \frac{\epsilon_s \epsilon_{s'} \langle\langle\psi_q\,|s\rangle \langle s\,|\psi_{q'}\rangle \langle\langle\psi_{q'}\,|s'\rangle \langle s'\,|\psi_q\rangle}{\varepsilon_q - \varepsilon_{q'}} .
$$

We are interested in the imaginary part of the perturbed eigenvalues, and, since the eigenstates, $|\psi_q\rangle$, are *real*, first order corrections never contribute to those terms. Considering now averages over disorder and writing $\langle\varepsilon'_q\rangle = \delta_q - i\gamma_q/2$, with δ_q, γ_q real, we obtain the average decay widths for the superradiant state

$$
\gamma_N = N\gamma - \gamma\frac{W^2}{48\Omega^2 N} \sum_{s=1}^N \sum_{q'=1}^{N-1} \frac{1}{\left(1 - \cos\frac{2\pi q'}{N}\right)^2 + \frac{N^2\gamma^2}{16\Omega^2}}
$$

$$
= N\gamma - \frac{\gamma W^2}{48\Omega^2} \sum_{q'=1}^{N-1} \frac{1}{\left(1 - \cos\frac{2\pi q'}{N}\right)^2 + \frac{N^2\gamma^2}{16\Omega^2}} , \quad (A5)
$$

and, for the subradiant ones, $q = 1, \ldots, N-1$,

$$
\gamma_q = \frac{\gamma W^2}{48\Omega^2 N} \sum_{s=1}^N \frac{1}{\left(\cos\frac{2\pi q}{N} - 1\right)^2 + \frac{N^2\gamma^2}{16\Omega^2}}
$$

$$
= \frac{\gamma W^2}{48\Omega^2} \frac{1}{\left(\cos\frac{2\pi q}{N} - 1\right)^2 + \frac{N^2\gamma^2}{16\Omega^2}} . \quad (A6)
$$

The maximum decay widths of the subradiant states are clearly γ_1 and γ_{N-1}, while the average of the subradiant

widths is

$$
\langle\Gamma_{sub}\rangle = \frac{\gamma W^2}{48\Omega^2(N-1)} \sum_{q=1}^{N-1} \frac{1}{\left(\cos\frac{2\pi q}{N} - 1\right)^2 + \frac{N^2\gamma^2}{16\Omega^2}} . \tag{A7}
$$

We finally define the critical disorder W_{cr} as the one at which

$$
\langle\Gamma_{sub}\rangle = \gamma,
$$

i.e. equals the single-site decay width γ.

Let us now apply first order perturbation theory to the superradiant state. For $W = 0$, the superradiant state is given by the extended state, Eq. (3), while, for $W \neq 0$, we can write

$$
|SR\rangle \simeq (1/\sqrt{N}) \sum_{k=1}^N |k\rangle + \sum_{q \neq 1} \frac{D_{1,q}}{\epsilon_1 - \epsilon_q} |\psi_q\rangle .
$$

From this expression we can compute the probability to be in the superradiant state when starting from the extended state as

$$
c_1 = \frac{1}{1 + \dfrac{W^2}{48\Omega^2 N} \displaystyle\sum_{s=1}^{N-1} \dfrac{1}{(1 + \cos(2\pi s/N))^2 + (\gamma N/4\Omega)^2}} . \tag{A8}
$$

Appendix B: Approximate formula for perturbative average width

Let us rewrite Eq. (A7) in the form

$$
\langle\Gamma_{sub}\rangle = \frac{\gamma W^2}{48\Omega^2} S_a , \tag{B1}
$$

where we have defined

$$
S_a = \frac{1}{N-1} \sum_{q=1}^{N-1} \frac{1}{\left(\cos\frac{2\pi q}{N} - 1\right)^2 + a^2} , \tag{B2}
$$

and

$$
a = \frac{N\gamma}{4\Omega} .
$$

Eq. (B2) can be put in integral form for sufficiently large N, that is $2\pi/N \ll 1$, as

$$
S_a = \frac{1}{2\pi} \int_0^{2\pi} dx \frac{1}{(\cos x - 1)^2 + a^2}
$$

$$
= \frac{\left(2a + 2\sqrt{4 + a^2}\right)^{1/2}}{a^{3/2}\sqrt{4 + a^2}} . \tag{B3}
$$

It is easy to show that Eq. (B3) has two different limits, namely

$$
S_a = \begin{cases} 1/(2a^{3/2}) & \text{for } a \ll 1, \\ \\ 1/a^2 & \text{for } a \gg 1. \end{cases} \tag{B4}
$$

Nevertheless, substituting a sum with an integral works only for very large N. For small $N < 100$, or, in general for a sufficiently small a value, it is more convenient approximating the sum with only two terms, namely those for which the denominator in Eq. (B2) is small. In detail, one has

$$1 - \cos(2\pi/N) \approx 2\pi^2/N^2 \text{ for } a < a_{cr} = 2\pi^2/N^2. \quad \text{(B5)}$$

This implies that, in this regime,

$$S_a = const \approx N^3/2\pi^4.$$

On the other hand, for $a_{cr} < a < 1$ (for all those N values for which $a_{cr} < 1$), one can approximate the sum with the integral and use the asymptotic behavior given in Eq. (B4). To summarize we have the following behavior:

$$S_a = \begin{cases} \dfrac{N^3}{2\pi^4} & \text{for } a \ll \dfrac{2\pi^2}{N^2}, \\[2mm] \dfrac{1}{2a^{3/2}} & \text{for } \dfrac{2\pi^2}{N^2} < a < 1, \\[2mm] \dfrac{1}{a^2} & \text{for } a \gg 1. \end{cases} \quad \text{(B6)}$$

These different regimes can be written in terms of physical parameters as follows:

$$\langle \Gamma_{sub} \rangle = \begin{cases} \dfrac{\gamma W^2 N^3}{96\pi^4 \Omega^2} & \text{for } \dfrac{N^3 \gamma}{8\pi^2 \Omega} \ll 1, \\[3mm] \dfrac{\gamma W^2}{12\gamma^{1/2}\Omega^{1/2}N^{3/2}} & \text{for } \dfrac{2\pi^2}{N^2} \ll \dfrac{N\gamma}{4\Omega} \ll 1, \\[3mm] \dfrac{W^2}{3N^2\gamma} & \text{for } \dfrac{N\gamma}{4\Omega} \gg 1. \end{cases} \quad \text{(B7)}$$

[1] G. S. Engel, T. R. Calhoun, E. L. Read, T.-K. Ahn, T. Mančal, Y.-C. Cheng, R. E. Blankenship, and G. R. Fleming, Nature **446**, 782 (2007).

[2] G. Panitchayangkoon, D. Hayes, K. A. Fransted, J. R. Caram, E. Harel, J. Wen, R. E. Blankenship, and G. S. Engel, PNAS **107**, 12766 (2010).

[3] M. Sarovar, A. Ishizaki, G. R. Fleming, and K. B. Whaley, Nat. Phys. **6**, 462 (2010).

[4] H. Hossein-Nejad and G. D. Scholes, New J. Phys. **12**, 065045 (2010).

[5] J. Strumpfer, M. Sener, and K. Schulten. J. Phys. Chem. Lett. **3**, 536 (2012).

[6] H. Fidder, J. Knoester, and D. A. Wiersma, J. Chem. Phys. **95**, 7880 (1991); J. Moll, S. Daehne, J. R. Durrant, and D. A. Wiersma, J. Chem. Phys. **102**, 6362 (1995).

[7] J. M. Moix, M. Khasin, and J. Cao, New J. Phys., 15, 085010 (2013).

[8] K. D. B. Higgins, S. C. Benjamin, T. M. Stace, G. J. Milburn, B. W. Lovett, and E. M. Gauger, arXiv:1306.1483

[9] M. Sarovar and K. B. Whaley, New J. Phys. **15**, 013030 (2013).

[10] A. Olaya-Castro, C. F. Lee, F. Fassioli Olsen, and N. F. Johnson, Phys. Rev. B **78**, 085115 (2008).

[11] J. Grad, G. Hernandez, and S. Mukamel, Phys. Rev. A **37**, 3835 (1988).

[12] F. C. Spano and S. Mukamel, J. Chem. Phys. **91**, 683 (1989).

[13] X. Hu, T. Ritz, A. Damjanovic, and K. Schulten, J. Phys. Chem. B **101**, 3854 (1997); X. Hu, A. Damjanovic, T. Ritz, and K. Schulten, PNAS **95**, 5935 (1998); T. Ritz, S. Park, and K. Schulten, J. Phys. Chem. B **105**, 8259 (2001).

[14] G. L. Celardo and L. Kaplan, Phys. Rev. B **79**, 155108 (2009); G. L. Celardo, A. M. Smith, S. Sorathia, V. G. Zelevinsky, R. A. Senkov, and L. Kaplan, Phys. Rev. B **82**, 165437 (2010).

[15] A. F. Sadreev and I. Rotter, J. Phys. A **36**, 11413 (2003).

[16] G. L. Celardo, P. Poli, L. Lussardi, F. Borgonovi, arXiv:1403.5660

[17] V. V. Sokolov and V. G. Zelevinsky, Nucl. Phys. **A504**, 562 (1989); Phys. Lett. B **202**, 10 (1988); I. Rotter, Rep. Prog. Phys. **54**, 635 (1991); V. V. Sokolov and V. G. Zelevinsky, Ann. Phys. (N.Y.) **216**, 323 (1992).

[18] R. H. Dicke, Phys. Rev. **93**, 99 (1954).

[19] M. O. Scully and A. A. Svidzinsky, Science **328**, 1239 (2010);

[20] S. Lloyd and M. Mohseni, New J. Phys. **12**, 075020 (2010).

[21] G. D. Scholes, Chem. Phys. **275**, 373 (2002).

[22] R. Monshouwer, M. Abrahamsson, F. van Mourik, and R. van Grondelle, J. Phys. Chem. B **101**, 7241 (1997).

[23] G. L.Celardo , F. Borgonovi, V. I. Tsifrinovich, M. Merkli, and G. P. Berman, J. Phys. Chem. C **116**, 22105 (2012).

[24] D. Ferrari, G. L. Celardo , G. P. Berman, R. T. Sayre, F. Borgonovi, J. Phys. Chem. C **118**, 20 (2014).

[25] P. W. Anderson, Phys. Rev. **109**, 1492 (1958).

[26] D. J. Heijs, V. A. Malyshev, and J. Knoester, Phys. Rev. Lett. **95**, 177402 (2005).

[27] G. L. Celardo, A. Biella, L. Kaplan, and F. Borgonovi Fortschr. Phys. **61**, No. 2-3, 250-260 (2013); A. Biella, F. Borgonovi, R. Kaiser, and G. L. Celardo, Europhys. Lett. **103** 57009 (2013).

[28] T. V. Shahbazyan, M. E. Raikh, and Z. V. Vardeny, Phys. Rev. B **61**, 13266 (2000).

[29] P. Rebentrost, M. Mohseni, I.Kassal, S. Lloyd, and A. Aspuru-Guzik, New J. Phys. **11**, 033003 (2009); P. Rebentrost, M. Mohseni, and A. Aspuru-Guzik, J. Phys. Chem. B **113**, 9942 (2009).

[30] M. B. Plenio and S. F. Huelga, New J. Phys. **10**, 113019 (2008); F. Caruso, A. W. Chin, A. Datta, S. F. Huelga, and M. B. Plenio, J. Chem. Phys. **131**, 105106 (2009).

[31] G. L. Celardo, F. M. Izrailev, V. G. Zelevinsky, and G. P. Berman, Phys. Lett B **659**, 170 (2008); G. L. Celardo, F. M. Izrailev, V. G. Zelevinsky, and G. P. Berman, Phys. Rev. E, **76**, 031119 (2007); G. L. Celardo, S. Sorathia, F.

M. Izrailev, V. G. Zelevinsky, and G. P. Berman, CP995, Nuclei and Mesoscopic Physics - WNMP 2007, ed. P. Danielewicz, P. Piecuch, and V. Zelevinsky.

[32] A. Rodríguez, V. A. Malyshev, G. Sierra, M. A. Martín-Delgado, J. Rodríguez-Laguna, and F. Domínguez-Adame, Phys. Rev. Lett. **90**, 027404 (2003); L. S. Levitov, Europhys. Lett., **9**, 83 (1989).

[33] F. M. Izrailev, A. A. Krokhin, and N. M. Makarov, Phys. Rep. **512**, 125 (2012).

[34] S. M. Vlaming, V. A. Malyshev, and J. Knoester, Phys. Rev, **79**, 205121 (2009).

[35] V. V. Temnov and U. Woggon, Phys. Rev. Lett. **95**, 243602 (2005).